BRAF and *DIS3* Mutations Associate with Adverse Outcome in a Long-term Follow-up of Patients with Multiple Myeloma

Eileen M. Boyle[1,2,3], Cody Ashby[1], Ruslana G. Tytarenko[1], Shayu Deshpande[1], Hongwei Wang[4], Yan Wang[1], Adam Rosenthal[4], Jeffrey Sawyer[1], Erming Tian[1], Erin Flynt[5], Antje Hoering[4], Sarah K. Johnson[1], Michael W. Rutherford[1], Christopher P. Wardell[1], Michael A. Bauer[1], Charles Dumontet[2], Thierry Facon[6], Sharmilan Thanendrarajan[1], Carolina D. Schinke[1], Maurizio Zangari[1], Frits van Rhee[1], Bart Barlogie[7], David Cairns[8], Graham Jackson[9], Anjan Thakurta[5], Faith E. Davies[3], Gareth J. Morgan[3], and Brian A. Walker[1,10]

ABSTRACT

Purpose: Copy-number changes and translocations have been studied extensively in many datasets with long-term follow-up. The impact of mutations remains debated given the short time to follow-up of most datasets.

Experimental Design: We performed targeted panel sequencing covering 125 myeloma-specific genes and the loci involved in translocations in 223 newly diagnosed myeloma samples recruited into one of the total therapy trials.

Results: As expected, the most commonly mutated genes were *NRAS, KRAS*, and *BRAF*, making up 44% of patients. Double-Hit and *BRAF* and *DIS3* mutations had an impact on outcome alongside classical risk factors in the context of an intensive treatment approach. We were able to identify both V600E and non-V600E *BRAF* mutations, 58% of which were predicted to be hypoactive or kinase dead. Interestingly, 44% of the hypoactive/kinase dead *BRAF*-mutated patients showed co-occurring alterations in *KRAS, NRAS*, or activating *BRAF* mutations, suggesting that they play a role in the oncogenesis of multiple myeloma by facilitating MAPK activation and may lead to chemoresistance.

Conclusions: Overall, these data highlight the importance of mutational screening to better understand newly diagnosed multiple myeloma and may lead to patient-specific mutation-driven treatment approaches.

Introduction

Multiple myeloma is a hematologic malignancy of plasma cells that afflicts around 30,000 people in the United States per year with a five-year survival rate of 47% (1). High-risk multiple myeloma (HRMM) is seen in up to 30% of newly diagnosed cases whose outcome, in contrast with the majority of multiple myeloma cases, has seen very little improvement over the past 15 years (2) with a median progression-free survival (PFS) of 1.8 years and overall survival (OS) of 2.6 years (3). There is, therefore, a clear need to identify these patients to apply relevant new approaches in their management.

The study of multiple myeloma has identified many genetic events that are associated with event-free survival (EFS) and OS. Some of these features occur with a greater frequency in HRMM cases, including translocations into the immunoglobulin (Ig) loci involving chromosomes 4 and 16, which define two etiological subgroups [t(4;14), 15%, and t(14;16), 5%; ref. 4]. Other instability mechanisms associated with HRMM include additional structural variations such as del(1p), and del(17p), jumping translocations of 1q, and secondary translocations to *MYC* at 8q24 (5–7).

A great deal is known about the genetics of multiple myeloma with over 800 genomes and 2,000 exomes sequenced (4, 6, 8–12). However, the prognostic impact of mutations has not been widely evaluated and available datasets have generally had a relatively short follow-up ranging from 22 to 25 months, with one dataset being up to 5.4 years (4, 11). These analyses have identified a diverse range of mutations that are associated with outcome, making it important to extend these observations over time in larger studies with robust diagnostic technologies.

Despite falling prices, it is not feasible to run whole-exome sequencing (WES) for every patient with multiple myeloma, and even then, many translocations outside of the capture region would be missed, requiring a combination of FISH or gene-expression profiling (GEP). Because this approach is time and cost prohibitive it has led to the adoption of targeted sequencing to generate data in a timely, cost-effective manner. This led us to design a custom myeloma-targeted panel, which provided rapid, fiscally responsible characterization of patient subgroups.

[1]Myeloma Center, Winthrop P. Rockefeller Cancer Institute, University of Arkansas for Medical Sciences, Little Rock, Arkansas. [2]INSERM 1052/CNRS 5286 Cancer Research Center of Lyon, Lyon, France. [3]Myeloma Research Program, New York University, Langone, Perlmutter Cancer Center, New York, New York. [4]Cancer Research and Biostatistics, Seattle, Washington. [5]Celgene Corporation, Summit, New Jersey. [6]Service des maladies du sang. Hôpital Claude Huriez, Lille University Hospital, Lille, France. [7]Department of Hematology and Medical Oncology, Tisch Cancer Institute, Icahn School of Medicine at Mount Sinai, New York, New York. [8]Clinical Trials Research Unit, Leeds Institute of Clinical Trials Research, Leeds, United Kingdom. [9]Northern Institute for Cancer Research, Newcastle University, Newcastle upon Tyne, United Kingdom. [10]Division of Hematology Oncology, Indiana University, Indianapolis, Indiana.

Note: Supplementary data for this article are available at Clinical Cancer Research Online (http://clincancerres.aacrjournals.org/).

E.M. Boyle and C. Ashby contributed equally to this article.

Corresponding Author: Brian A. Walker, Indiana University—Purdue University Indianapolis, Indiana University, 975 West Walnut Street, IB 544B, Indianapolis, IN 46202. Phone: 317-278-7733; Fax: 317-274-0396; E-mail: bw75@iu.edu

Clin Cancer Res 2020;26:2422–32

doi: 10.1158/1078-0432.CCR-19-1507

Translational Relevance

Identifying diagnostic, prognostic, and theragnostic factors is key in the modern management of patients with cancer, including myeloma. Here, we designed a next-generation sequencing targeted capture over 125 myeloma-specific genes and the canonical translocation loci to identify the mutations, copy number, and translocation makeup of newly diagnosed patients with myeloma and use this to identify independent features associated with outcome. Using this approach, we were able to identify different markers as well as their interaction with one another and both confirm previous findings and identify new changes associated with outcome. The originality of this dataset resides in the extensiveness of features analyzed and the long-term follow-up of this trial population. Therefore, the novel markers identified will help add precision to the management of newly diagnosed patients with myeloma treated in an intensive setting.

We evaluated this panel on 223 patients with newly diagnosed multiple myeloma (NDMM) included in the total therapy (TT) trials and correlated results to both gene expression and clinical data, with the ultimate aim of this work being to effectively characterize patients with NDMM and identify the impact of mutations long term.

Materials and Methods

Patients and Samples

A total of 223 previously untreated patients with NDMM recruited to the TT trials between February 2004 and August 2017 were included after written informed consent. The sample collection protocol was approved by the UAMS Institutional Review Board (protocol #2012–12). The TT trials are a series of phase II and III, alkylator heavy, double transplant–based clinical trials for first-line myeloma treatment that all include both proteasome inhibitors and immunomodulatory drugs (IMiD). A summary of the treatments received may be found in Supplementary Fig. S1. Eighty-five of these samples were previously used as a validation of the Double-Hit model (3). Sample processing may be found in the Supplementary Methods. This study was performed in accordance to the 1964 Helsinki Declaration.

Sequencing

Panel Design. Genes and chromosomal regions relevant to the biology, prognosis, and treatment of multiple myeloma were identified. This information was used to design and implement a targeted panel to identify common and important genomic abnormalities in multiple myeloma. Probes captured exonic regions for the relevant genes ($n\sim125$), including $\pm$ 10 base pairs (bp), to include splice site variants (Supplementary Table S1). Single-nucleotide polymorphisms (SNP) with a minor allele frequency >0.35 were captured in regions of interest to infer copy number using allelic imbalance combined with read depth ratio. In this way both deletions and gains were confidently assayed. SNPs in GC-rich regions were avoided to prevent hybridization artefacts and low depth problems. To identify Ig translocations, the V, D, and J segments along with entire constant region were tiled (81.8–90.2 Mb, 17.4–32.6 Mb, 106.0–107.3 Mb for *IGK*, *IGL*, and *IGH*, respectively (4, 13, 14). *MYC* translocations were also detected by tiling 2 Mb upstream and downstream of *MYC* (126.3–130.8 Mb).

Targeted Sequencing. The panel was divided into a translocation panel and a mutation/copy-number panel to provide high-depth coverage for mutation analysis (0.6 Mb), while providing lower-depth sequencing of translocation regions (4.2 Mb).

Each patient had their tumor DNA from bone marrow and control DNA from peripheral blood sequenced, to identify somatic mutations, copy-number changes, and translocations. 50 ng of DNA was used to prepare libraries using the HyperPlus kit (Kapa Biosystems) and split for hybridizing to both mutation and translocation captures (SeqCap EZ target enrichment; Nimblegen), after which mutation and translocation captures were combined. The HiSeq 2500 or NextSeq500 (Illumina) were used for sequencing with 75 bp paired-end reads. The median value of the mean coverage of each sample was 135x and 452x for translocations and mutations, respectively.

Data analysis

bcl2fastq was used for demultiplexing and BWA mem (v. 0.7.12) for alignment to Ensembl (GRCh37/hg19) human reference genome. Strelka (v.1.0.14) was used for variant calling and single-nucleotide variants (SNV) were filtered using fpfilter (https://github.com/ckandoth/variant-filter). Indels were filtered using a 10% variant allele frequency (VAF) cutoff. Variants were annotated using Variant Effect Predictor (v.85). To determine copy number, a normalized depth comparison between tumor and control samples was used and segments of SNP variance were used to identify regions of chromosomal deletion and gain. Copy number was manually normalized on the basis of the ratio and SNP allele calls using the best fitting chromosomes with the least variance (usually chromosome 2 or 10). Data were visualized using a custom built R-Shiny application. Intra- and inter-chromosomal rearrangements were called using Manta (v0.29.6) with default settings and the exome flag specified. QC metrics estimated the cross-sample contamination of samples using homozygous SNPs in the germline with 95% or higher VAF examined in the tumor sample. A VAF density plot on those SNPs was generated, as well as reporting the minimum, maximum, and median of their values in the germline and tumor (Supplementary Fig. S2).

Validation and comparison datasets

SNVs. SNVs were compared and validated using seven samples (Horizon Diagnostics) with known SNVs and VAF. The VAF of mutations found in the validation samples matched those found on the panel with $r^2 = 0.93$ (Supplementary Fig. S3).

FISH. Copy-number data generated from the sequencing panel were validated against existing FISH data for del(1p) [1p13 FISH vs. 1p12 (*FAM46C*) seq.], gain (3 copies)/amp (4 copies or more) (1q21), del (13q) (*D13S31* vs. *RB1*), and del(17p) (*TP53*). Plots of comparisons between FISH and sequencing data are shown with specificities and sensitivities of each region at the 20%, 25%, 40%, and 50% FISH cutoff (Supplementary Fig. S4 and Supplementary Table S2). An additional comparison for *TP53* was made using the prognostic cutoff 55% (15). All deletions identified by FISH were identified using the targeted panel. Five additional deletions were called using the panel, 3/5 of them having a del(17p) in at least 20% of cells by FISH (Supplementary Figs. S5 and S20).

Comparison Dataset. Gene mutations were compared with the MGP dataset (n = 1,273; ref. 3) available in the European Genome-Phenome Archive under accession numbers EGAS00001001147, EGAS00001000036, and EGAS00001002859, or at dbGAP under accession number phs000748.v5.p4.

Gene-expression profiling

Total RNA from plasma cells was used for GEP using U133 Plus 2.0 microarrays (Affymetrix). Raw signals were MAS5 normalized using the Affymetrix Microarray GCOS1.1 software. GEP70, TC classification, and molecular clusters were derived as previously published (16).

BRAF mutation analysis

The predicted functions of *BRAF* mutations were determined using the Clinical Knowledgebase (CKB) database (17) using the mutations present in the MGP dataset (n = 103; ref. 8) and this dataset (n = 26).

Data availability

Sequencing data and expression data have been deposited in the European Genome-Phenome Archive under the accession numbers EGAS00001003223 and EGAD00001004117.

Statistical analysis and additional methods may be found in Supplementary Methods.

Results

Patient characteristics

A total of 223 patients were sequenced and included in the study. Overall, they were representative of a fit–newly diagnosed population. The median follow-up time from diagnosis was 8.14 years [95% confidence interval (CI), 7.39–9.02]. The median OS was not met at the time of analysis and the 8-year OS was 61% (95% CI, 54%–69%). The median EFS was 6.16 years (95% CI, 5.18–7.75). A summary of patient characteristics may be found in **Table 1**.

Table 1. Summary of patient's characteristics and comparability to the complete TT trial population.

	223-Baseline study	Combined TT3a-3b-4-4like-5a-5b-6
Number of patients	223	1039
Inclusion dates	02/2004 to 08/2017	02/2004 to 08/2017
Median follow-up	8.14 years (95% CI, 7.39–9.02)	8.35 years (95% CI, 8.00–8.63)
Median EFS	6.16 years (95% CI, 5.18–7.75)	4.8 years (95% CI, 52%–58%)
8-year OS	61% (95% CI, 54%–69%)	42% (95% CI, 39%–45%)
Median age (y)	59 (range, 30–75)	61 (range, 30–76)
Sex ratio M:F	1.8:1	1.6:1
Ethnicity (%)		
White	88% (n = 197)	86.8% (n = 902)
African-American	10% (n = 22)	9.7% (n = 101)
Other	2% (n = 4)	3.5% (n = 36)
ISS (%)		
I	26.5% (n = 59)	34.0% (n = 352)
II	43.5% (n = 97)	40.2% (n = 416)
III	30.0% (n = 67)	25.8% (n = 267)
R-ISS (%)		
I	17.0% (n = 38)	
II	67.7% (n = 151)	
III	15.2% (n = 34)	
GEP70 high risk (%)	16.1% (n = 36)	15.9% (n = 165)

The incidence of translocation and copy number were in keeping with previously published data. *MYC* translocations were identified in 26% of cases. They involved the Ig locus in 39% of cases and non-Ig partners in 61% of cases. The breakpoints were within the previously published hotspots (Supplementary Fig. S6A). *MYC* deletions and gain were seen in 16% and 28% of patients, respectively. An example may be seen in Supplementary Fig. S7. Overall, *MYC* events were seen in 47% of patients. A summary of the translocations and comparison to the MGP (3) data may be found in Supplementary Table S11.

The most commonly mutated genes were *KRAS* (23% of patients), *NRAS* (17% of patients), and *BRAF* (12% of patients) (**Fig. 1A**), in keeping with previously published datasets. The incidence of mutations was similar to the MGP study (Supplementary Table S4).

Exome sequencing identifies an APOBEC-derived mutational signature in approximately 80% of t(14;16) samples (18). We performed nNMF analysis on our targeted sequencing to determine whether we could identify an APOBEC signature, which was seen in seven patients (3.2%), five of which had a t(14;16) and one a t(14;20) translocation (**Fig. 1C** and Supplementary Fig. S8). Both frequency and enrichment for the MAF subgroups were in keeping with previous reports (18).

Interactions between genomic abnormalities and Double-Hit myeloma

Pearson's correlation identified a significant correlation between *CYLD* mutations and deletions ($r = 0.31$, $P = 2.07 \times 10^{-7}$), *TRAF3* mutations and deletions ($r = 0.34$, $P = 1.5 \times 10^{-7}$), and *TP53* mutations and deletions ($r = 0.32$, $P = 1.12 \times 10^{-6}$), as previously reported (4, 8). *ATM* mutations were positively correlated with the t(14;16) subgroup ($r = 0.40$, $P = 3.33 \times 10^{-7}$) and the presence of an APOBEC signature ($r = 0.62$, $P = 8.66 \times 10^{-10}$). There was no significant negative correlation between *DIS3* mutations and hyperdiploidy (HRD; $r = -0.11$, $P = 0.09$) in this dataset, although they were positively correlated to the presence of t(4;14) ($r = 0.21$, $P = 0.0005$). On the other hand, del(13q) was negatively correlated to HRD ($r = -0.26$, $P = 0.0001$; **Fig. 1B**).

We identified 8.1% patients with Double-Hit [ISS III plus amp(1q) or biallelic inactivation of *TP53*] that is not significantly different to the 6.1% of patients previously described. Double-Hit was associated with both an adverse EFS [median: 24.6 months (95% CI, 10.6–42.7) vs. 6.77 years (95% CI, 5.60–∞; $P < 0.0001$)] and OS [37.3 months (95% CI, 32.3–∞) vs. 64% at 8 years (95% CI, 57%–73%; $P < 0.0001$)]. Interestingly, when analyzing the impact of Double-Hit in the TT population, which received two autologous stem cell transplants (ASCT), the impact of Double-Hit was still significant. This is of particular interest in a double-ASCT population (Supplementary Fig. S9) identifying a population that still has a dire outcome despite intensive treatment.

Survival analysis identifies that *BRAF* and *DIS3* mutations are associated with an adverse outcome with long-term follow-up

Univariate Analysis. Power estimation was performed (Supplementary Fig. S10). The results of univariate analyses for EFS and OS for molecular features are shown in **Fig. 2**. Overall, this dataset behaved as expected with del(12p), del(17p), gain/amp(1q), and del(1p) being significantly associated with both adverse EFS and OS. Trisomy(9) and trisomy(19) were associated with a better EFS and OS and trisomy(2) and trisomy(5) resulted in a better EFS. The other trisomies (3, 15

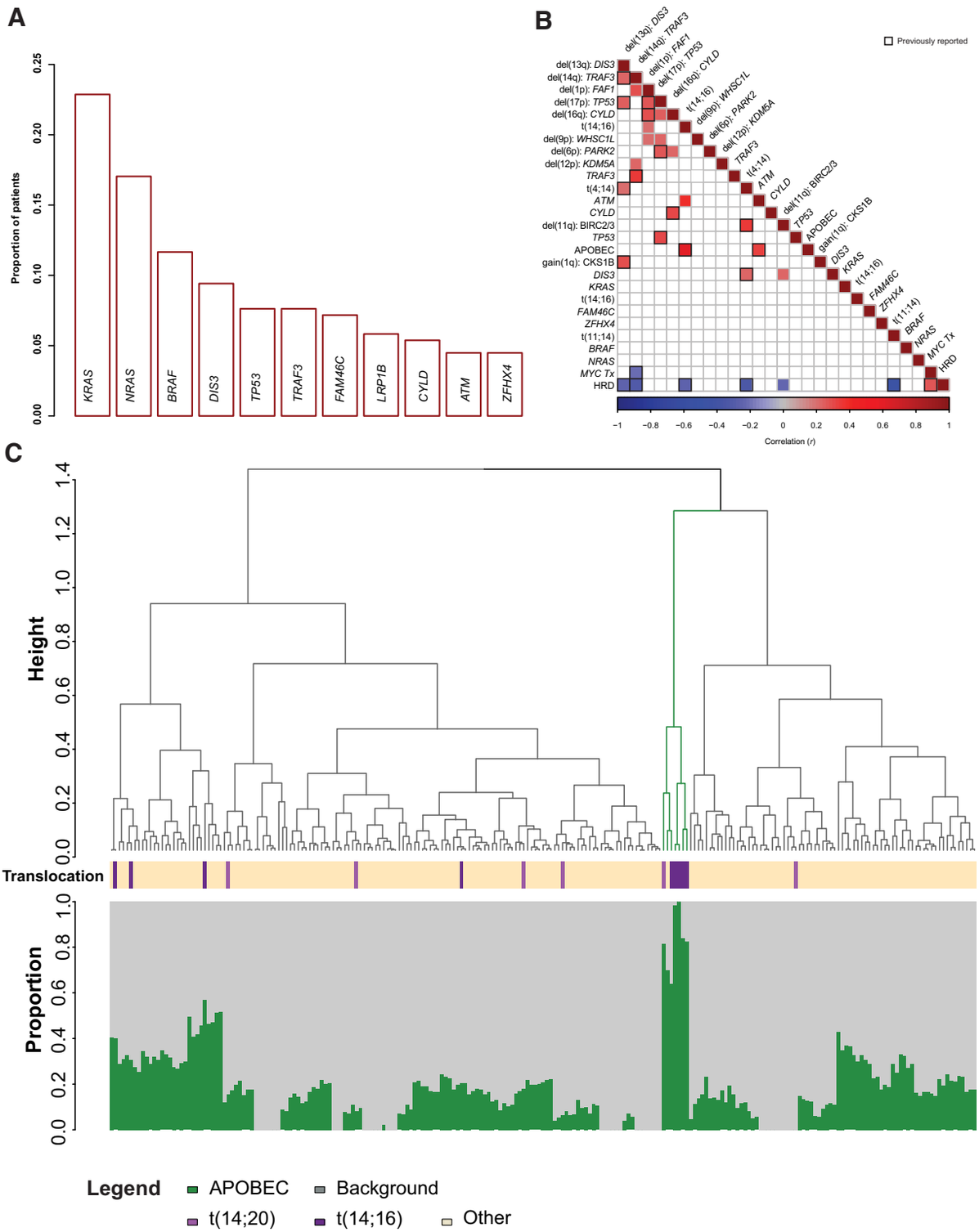

Figure 1.

General features of the cohort. **A,** The proportion of patients with each mutation. **B,** Correlation plot representing the different significant interactions. **C,** Dendrogram of the nNMF identifying an APOBEC signature among the 223 TT baseline samples using the targeted panel.

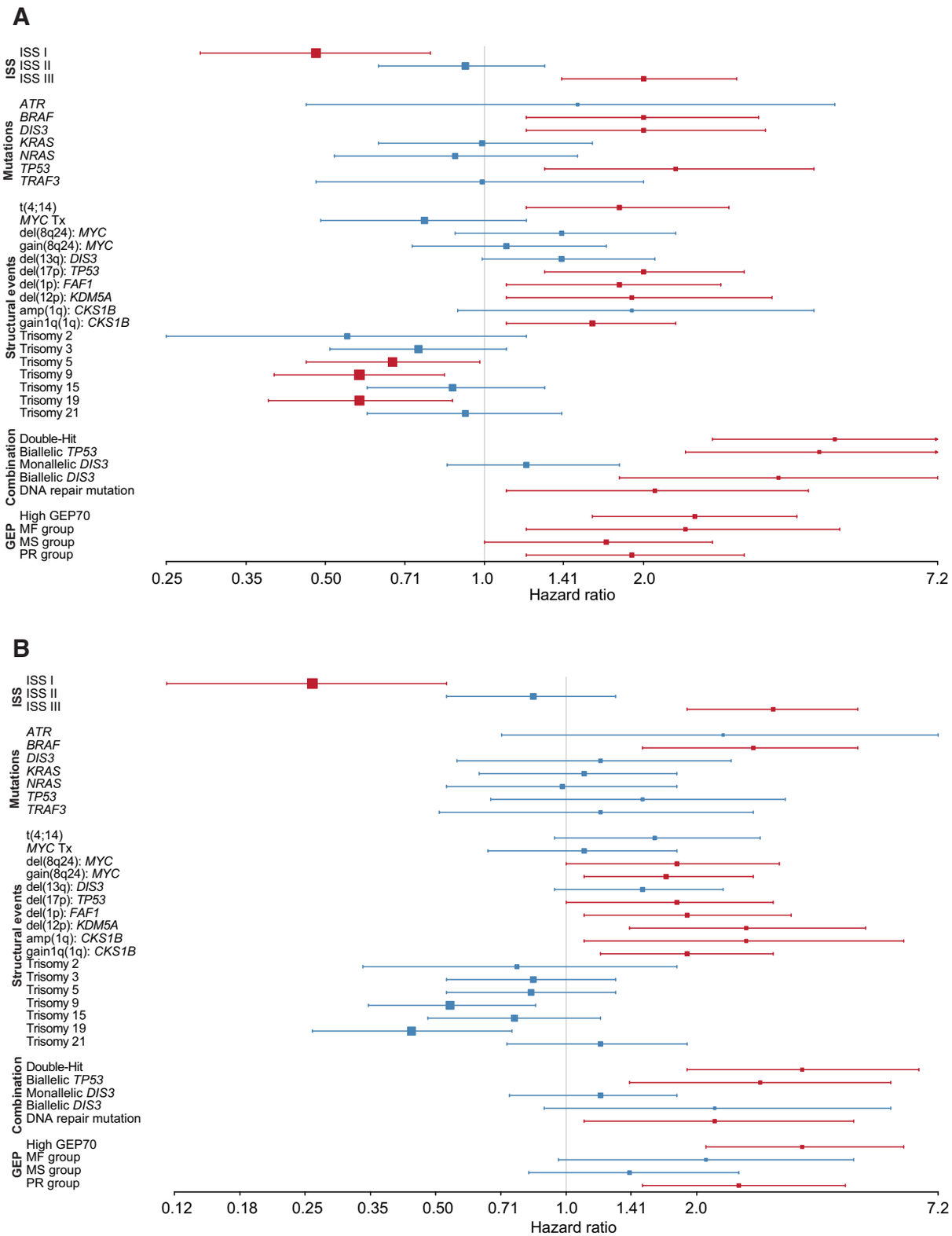

Figure 2.

Summary of the univariate analysis. **A,** EFS. **B,** OS. Forest plots representing the result of the univariate analysis. In red, those that were significantly associated with outcome at the level of $P < 0.05$; in blue, the non-significant variables.

and 20) had no impact on outcome. Sixteen percent of patients were considered as high risk according to the GEP70 score and they had a worse outcome than standard-risk patients both in terms of EFS (HR, 2.5; 95% CI, 1.6–3.9; $P < 0.0001$) and OS (HR, 3.5; 95% CI, 2.1–6; $P < 0.0001$) (Supplementary Fig. S11). The PR subgroup was also associated with both short EFS and OS whereas the MF and MS subgroup were associated with a short EFS. On the basis of their ISS, 26.5%, 43.5%, and 30% of patients were considered ISS I, ISS II, and ISS III, respectively, with an HR of death of 2.7 (95% CI, 1.2–5.9; $P = 0.01$) and 6.04 (95% CI, 2.8–13; $P < 0.0001$) for ISS II and III, respectively, in comparison with ISS I. *MYC* translocations, gains, and deletions were associated with a difference in OS in this dataset, but not EFS (Supplementary Fig. S6). In terms of mutations, *BRAF* mutations were associated with an adverse EFS (HR, 2; 95% CI, 1.2–3.3; $P = 0.009$) and OS (HR, 2.7; 95% CI, 1.5–4.7; $P = 0.0007$) (Supplementary Fig. S16A and S16B). *TP53* and *DIS3* mutations were associated with a worse EFS (HR, 2.3; 95% CI, 1.3–4.2; $P = 0.0065$ and HR, 2; 95% CI, 1.2–3.5; $P = 0.009$, respectively) but not OS (HR, 1.5; 95% CI, 0.67–3.2; $P = 0.34$ and HR, 1.2; 95% CI, 0.56–2.4; $P = 0.68$, respectively). We went on to test combinations of markers previously published such as DNA repair pathway mutations (4) and bi-allelic *TP53* (3). As previously shown (4), DNA repair pathway mutations defined by the presence of an *ATM* or *ATR* mutation were associated with an adverse outcome in terms of EFS (HR, 2.1; 95% CI, 1.1–4.1; $P = 0.023$) and OS (HR, 2.2; 95% CI, 1.1–4.6; $P = 0.033$), as was bi-allelic *TP53* (HR, 4.3; 95% CI, 2.4–7.7; $P < 0.0001$) and OS (HR, 2.8; 95% CI, 1.4–5.6; $P = 0.004$). There was no significant impact of IGL translocations on outcome (Supplementary Fig. S12). These data are summarized in Supplementary Table S5.

Multivariate analysis identifies mutations of *BRAF* and *DIS3* as independently associated with prognosis

We went on to perform a multivariate analysis using all the genetic features with $P < 0.1$.

For EFS, a protective effect was associated with trisomy(19). An adverse association was seen for Double-Hit, del(1p)(*FAF1*), t(4;14), del(12p)(*KDM5A*), and mutations of *BRAF* and *DIS3* (Corrected $C_{index} = 0.689$). Similarly, for OS, trisomy(19) was associated with a positive effect, whereas an adverse association was seen with Double-Hit, del(1p)(*FAF1*), del(12p)(*KDM5A*), gain(8q24) (*MYC*), and mutations of *BRAF* (Corrected $C_{index} = 0.73$). With the long follow-up there was consistency between markers in the multivariate analysis of EFS and OS, with the exception of *MYC* gains and mutation of *DIS3*, indicating a high reliability in the dataset. A summary of the multivariate may be found in **Fig. 3** and Supplementary Tables S6 and S7.

We tested the solidity of this analysis by repeating the analysis using classical risk factors and previously published models such as the IFM2009 model (20) and GEP70 (16) (Supplementary Figs. S13–S15). *DIS3* mutations and *BRAF* mutations retained their prognostic significance, irrespective of other high-risk features.

DIS3 mutations and biallelic *DIS3* events are associated with poor prognosis in multiple myeloma

In our dataset, we identified 21 patients (9.4%) with a *DIS3* mutation. The majority of the mutations were missense and were located throughout the gene suggesting that they were inactivating (**Fig. 4A**), although a hotspot is present at amino acid R780. Mutations in *DIS3* were associated with a worse EFS (HR, 2; 95% CI, 1.2–3.4; $P = 0.01$) but not OS. A similar trend was seen in the Myeloma XI dataset and the MGP (Supplementary Fig. S17). Biallelic events were seen in 11 (5%) patients, mostly consisting of deletions and mutations (91%, $n = 10/11$). There was no case of biallelic deletion. Bialleleic *DIS3* events had a stronger association with EFS (HR for progression of 3.6; 95% CI, 1.8–7.2; $P < 0.0001$) than monoallelic events (HR of 1.2; 95% CI, 0.85–1.8; $P = 0.27$ (**Fig. 4B–C**).

BRAF non-V600E mutations comprise kinase dead variants that were associated with adverse outcome, and may lead to increased MAPK activation through CRAF via co-occurring *KRAS* and *NRAS* mutations

BRAF mutations were associated with an adverse outcome in this cohort (Supplementary Fig. S16A and S16B). Forty-six percent ($n = 12/26$) were at the classical V600E hotspot (**Fig. 5A**). When comparing the impact of the non-V600E versus the V600E patients, for EFS especially, most of the prognostic impact appeared to driven by non-V600E mutations [1.3 years (0.58–∞) vs. 5.6 years (2.46–∞), $P = 0.02$ for EFS; 3.12 years (1.21–∞) vs. 8.62 years (5.73–∞), $P = 0.08$ for OS] (Supplementary Fig. S16C–S16F).

From a functional perspective, *BRAF* mutations can be sub-divided into activating or nonactivating, based on information from other cancers. Using the CKB database, we were able to dissect the non-V600E mutations into activating ($n = 5$), inactivating ($n = 8$), and unknown ($n = 1$) (Supplementary Table S8). The outcome of patients with the inactivating mutations was worse (HR, 6.4; 95% CI, 2.74–15; $P < 0.0001$) than those who had an activating mutation (HR, 2.1; 95% CI, 1.05–4.2; $P = 0.04$), which in turn was worse than those who did not have a *BRAF* mutation (**Fig. 5B** and **C**). Similar trends were confirmed in the MGP dataset subset of patients who received an ASCT (OS, $P = 0.008$) (Supplementary Fig. S17).

To explore this further, we expanded this analysis ($n = 26$) using the MGP dataset ($n = 103$). Combined, 43% (56/129) were V600E mutations, 11% (14/129) were predicted to be activating, 8.5% with hypoactive (11/129), 25% kinase dead (32/129), and 12.5% unknown (16/129).

In melanoma, inactivating mutations often co-occur with other MAPK alterations such as *NRAS or KRAS* mutations, *NF1* biallelic inactivation or *PTPN11* mutations, and contribute to increased MAPK signaling through enhanced binding and recruitment of CRAF (20). We hypothesized that the adverse outcome associated with inactivating *BRAF* mutations in myeloma is due to increased MAPK signaling, in which case co-occurring *NRAS* or *KRAS* mutations would need to be present in the same clone.

NRAS, KRAS, and *BRAF* mutations are believed to be mutually exclusive (4, 8) in multiple myeloma. In most cases, these three mutations were also mutually exclusive (Supplementary Fig. S18 A–S1B); however, inactivating *BRAF* mutations co-occurred more frequently with *NRAS, KRAS*, or activating *BRAF* mutations than expected, reaching 44% of patients with inactivating *BRAF* mutations ($P = 0.0018$) (**Fig. 5E**). To determine whether the co-occurring mutations were present in the same clone, we calculated the cancer clonal fraction (CCF) mutations and, based on the resulting proportions, assessed whether they were in the same clone. We identified that 68% ($n = 13/19$) of samples with an inactivating *BRAF* mutation had a co-occurring *NRAS/KRAS* mutation in the same clone and 32% ($n = 6/19$) could not be determined from the data (**Fig. 5F** and Supplementary Fig. S18C and S18D).

Discussion

The incorporation of the complete spectrum of genomic lesions from translocation to mutations, including copy-number changes,

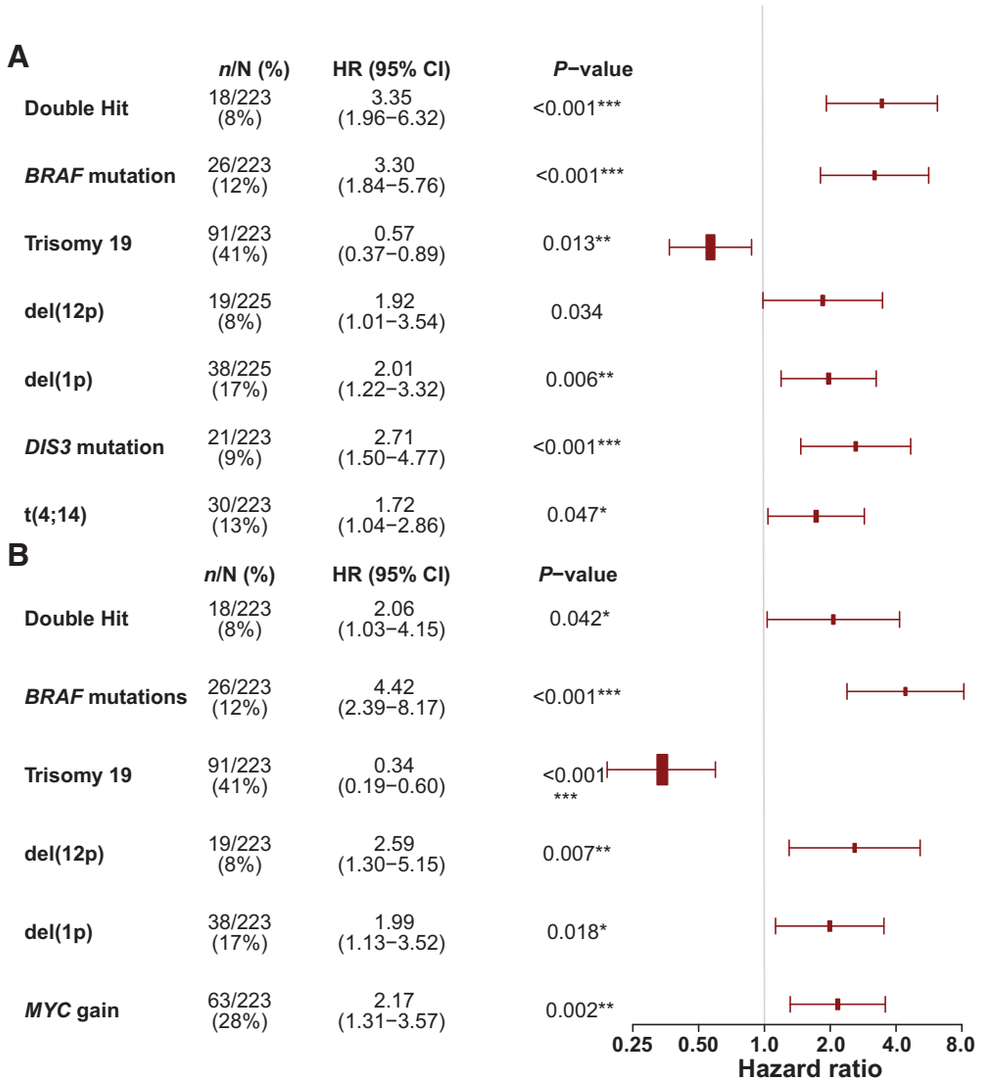

Figure 3.
Multivariate analysis. Forest plots representing the results of the multivariate analysis for (**A**) EFS and (**B**) OS.

is required to gain insight and accurately predict outcome in multiple myeloma. Using multiple techniques to determine these factors is both labor intensive, time consuming, and yields high failure rates given the amount of tumor cells required (21). Next-generation sequencing has helped unravel the genetic complexity of multiple myeloma but cost and time are often setbacks in a clinical setting. Many targeted approaches have been developed, some specific (22, 23) and some applicable (24) to multiple myeloma, but most do not take into account the Ig loci, thus requiring combinations with other tests such as FISH or GEP to identify translocations. Like Bolli and colleagues (23), our approach offers a complete view of translocations, CNA, and mutations. The set of genes in this capture largely overlaps the Sanger capture but given our wide *MYC* tiling we offer a better understanding of the complex rearrangements that occur on 8q24. Finally, given the size of this capture, we are also able to identify an APOBEC signature, that has also demonstrated prognostic significance in multiple myeloma (18).

Here, we show that an increased follow-up of patient outcome data combined with targeted sequencing can identify consistent genomic markers associated with inferior outcome. We identified the classical cytogenetic abnormalities, such as t(4;14), del(1p), and del(12p), as affecting outcome, as well as the more recently defined Double-Hit myeloma. In addition, we identify that mutations in *BRAF* and *DIS3* are prognostically implicated in the outcome of patients with myeloma in an intensive setting.

In the MGP dataset, we have previously shown that Double-Hit myeloma resulted in a worse outcome for PFS and OS, irrespective of the treatment used, but these patients mostly had a single ASCT. ASCT is the standard of care for all NDMM patients age $\leq$ 65 years, and before the era of novel agents, ASCT proved beneficial on OS (25). Double transplants were subsequently investigated and deemed

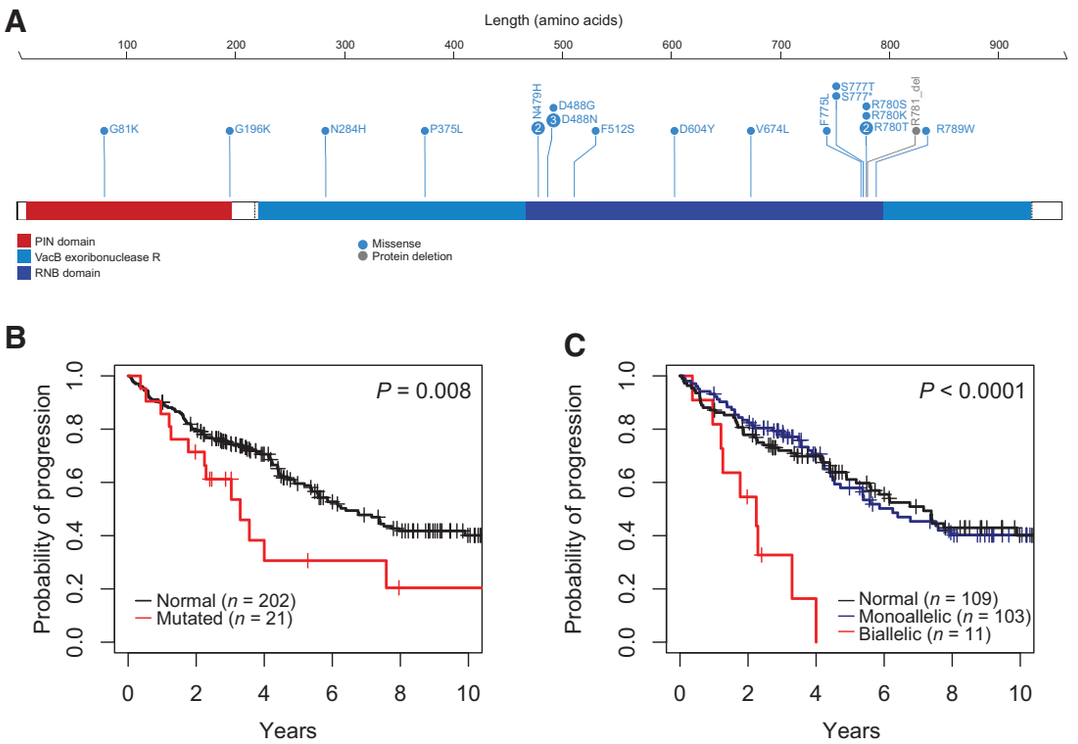

Figure 4.

DIS3 mutations. **A,** Distribution of *DIS3* mutations throughout the gene. **B,** *DIS3* mutations are associated with an adverse EFS. **C,** Biallelic *DIS3* inactivation is associated with a worse outcome than monoallelic inactivation.

safe (26–29), and two randomized trials confirmed the benefit of double versus single transplant in terms of OS (25). In this dataset, all patients received a double ASCT, but despite this, Double-Hit patients still perform badly, although they have a slightly better outcome than was seen in the MGP data (20.7 months; 95% CI, 17.4–20.6), with a 16-month improvement in their outcome.

BRAF mutations were seen in 11% of patients with myeloma and were associated with a poor outcome. *BRAF* is mutated in numerous cancers and the substitution of a valine (V) for a glutamic acid (E) residue at position 600 in the kinase domain is the most common *BRAF* mutation (30). This mutation mimics the phosphorylation of the activation loop, thereby inducing constitutive BRAF kinase activation. $BRAF^{V600E}$ mutations are present in 50% of melanoma patients and 2% of patients with non–small cell lung cancer (NSCLC). In NSCLC, they are associated with a shorter OS and resistance to cisplatinum chemotherapy (31). The clinical significance of $BRAF^{V600E}$ in multiple myeloma has been characterized in two previous studies where seven patients with myeloma with $BRAF^{V600E}$ had significantly shorter OS and an increased incidence of extra medullary disease (57% vs. 17%) compared with wild-type *BRAF* (32). More recently Rustad and colleagues (33) reported a good response to broad acting drugs and no relation to prognosis among eleven $BRAF^{V600E}$-mutant patients.

Fifty-four percent of the *BRAF* mutations seen in this dataset were non-V600E and is a similar rate to that seen in NSCLC (34, 35) and other multiple myeloma datasets (36). The biology of these non-V600E mutants is heterogeneous, with some leading to high kinase activity (class I and II) and Ras independence whereas others are hypoactive or kinase dead (class III), variants but nonetheless these still impact the MAPK pathway through CRAF heterodimerization (37, 38). In our dataset, the hypoinactive/kinase dead variants were more likely to co-occur with a *KRAS* or *NRAS* mutation which has also has been previously described by Lionetti and colleagues (36). In melanoma, biallelic *NF1* inactivation or *PTPN11* activation have also been linked to MAPK activation through inactive *BRAF* mutants (36, 39), but these are rare events in multiple myeloma and they were not associated with non-$BRAF^{V600E}$ mutants (Supplementary Fig. S19).

$BRAF^{V600E}$ mutations in melanoma are sensitive to the BRAF inhibitors vemurafenib and dabrafenib. Case reports (40, 41) and clinical trials (42) also support the use of vemurafenib in this setting. These drugs are not effective against non-$BRAF^{V600E}$ mutations, but could be targeted using MEK inhibitors.

In other cancers, the presence of concomitant NRAS/KRAS and BRAF kinase dead mutations results in chemoresistance (34, 43). Identifying these non-$BRAF^{V600E}$ mutants would not only help identify patients who should not receive BRAF inhibitors but also patients who would not benefit from intensive alkylator heavy regimens. The adverse outcome of these patients in this dataset could suggest that heavily treating these patients may be deleterious and may suggest they would benefit from alkylator-free regimens, thus explaining some of the outcome discrepancies in the literature (33).

The prognostic impact of chromosome 13 has been long debated. Forty percent of patients have a del(13q) either by a monosomy 13 (35%) or a simple loss of 13q (44). Del(13q) was found to be associated with a short outcome in many studies, before the associations between t(4;14) and del(13q) were made (45). *DIS3* is located on chromosome

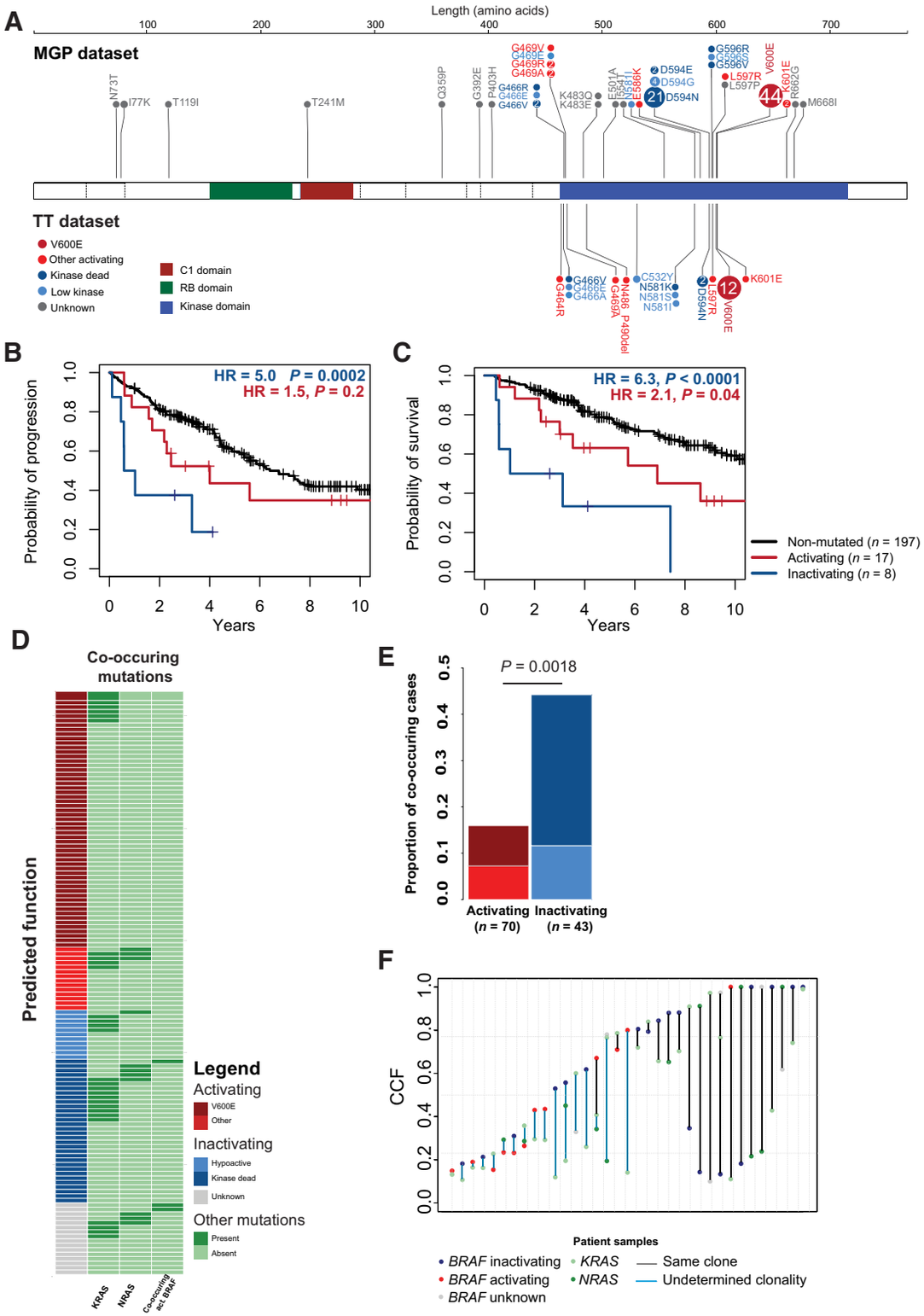

Figure 5.

Inactivating *BRAF* mutations affect outcome and co-occur with *NRAS* or *KRAS* mutations. **A,** Stick plot representing the locations of the different *BRAF* mutations in the MGP dataset (top) and TT dataset (bottom). Differential impact of *BRAF* mutations depending on predicted function on EFS (**B**) and OS (**C**). **D,** The spectrum of *BRAF* mutations with co-occurring mutations. **E,** The proportion of cases with co-occurring MAPK (*NRAS/KRAS*/activating *BRAF* mutations) depending on their predicted *BRAF* function. **F,** CCF of MAPK mutations to determine clonality.

13 and as such is frequently deleted, as well as being mutated in multiple myeloma (4, 8). More recently, *DIS3* germline variants have been described in familial cases of plasma cell disorders (46). Combined, we saw *DIS3* events in 53% of cases and bi-allelic events in 5%. We identified an association with poor outcome and bi-allelically affected *DIS3*, which may suggest that *DIS3* is a tumor-suppressor gene. However, the majority of *DIS3* mutations are missense and not nonsense or frameshift mutations; further, the mutations are clustered at particular codons that is not typical of a tumor-suppressor gene and may suggest an oncogenic potential for DIS3. In this respect, the mutations may cause a change of function, as has recently been suggested in yeast where point mutations are associated with genome instability (47). Given the role of DIS3 in RNA processing (48), it is possible that complete inactivation of both alleles is lethal, as has been seen for *SF3B1* (47).

BRAF and *DIS3* mutations have an impact on outcome alongside classical risk markers in the context of the TT trials. We were able to identify both $BRAF^{V600E}$ mutations and non-V600E *BRAF* mutations, 58% of which were predicted to be hypoactive or kinase dead. Interestingly, 44% of the hypoactive/kinase dead *BRAF* patients showed co-occurring mutations in *KRAS* or *NRAS*, suggesting that they play a role in the oncogenesis of multiple myeloma by facilitating MAPK activation by upstream mutated factors through CRAF. These data highlight the importance of mutational screening to better understand NDMM and may lead to patient-specific mutation-driven treatment approaches.

Disclosure of Potential Conflicts of Interest

E. Flynt is an employee/paid consultant for and holds ownership interest (including patents) in Bristol-Myers Squibb. A. Thakurta is an employee/paid consultant for and holds ownership interest (including patents) in Celgene. D.A. Cairns reports receiving commercial research grants from Celgene Corporation, Merck Sharpe&Dohme, and Amgen. G.H. Jackson reports receiving speakers bureau honoraria from Takeda, Celgene, Amgen, J&J, and Seattle Genetics. F.E. Davies is an employee/paid consultant for Celgene, Janssen, Amgen, Roche, Abbvie, Takeda, Sanofi, GlaxoSmithKline, and Bristol-Myers Squibb. No potential conflicts of interest were disclosed by the other authors.

Authors' Contributions

Conception and design: E.M. Boyle, C. Ashby, B. Barlogie, G.J. Morgan, B.A. Walker
Development of methodology: E.M. Boyle, H. Wang, Y. Wang, E. Tian, B. Barlogie, B.A. Walker
Acquisition of data (provided animals, acquired and managed patients, provided facilities, etc.): E.M. Boyle, S. Deshpande, J. Sawyer, E. Tian, E. Flynt, S.K. Johnson, M.W. Rutherford, S. Thanendrarajan, C.D. Schinke, F. van Rhee, B. Barlogie, D. Cairns, G. Jackson, A. Thakurta, F.E. Davies, G.J. Morgan, B.A. Walker
Analysis and interpretation of data (e.g., statistical analysis, biostatistics, computational analysis): E.M. Boyle, C. Ashby, H. Wang, Y. Wang, A. Rosenthal, C.P. Wardell, M.A. Bauer, M. Zangari, B. Barlogie, D. Cairns, G. Jackson, F.E. Davies, G.J. Morgan, B.A. Walker
Writing, review, and/or revision of the manuscript: E.M. Boyle, C. Ashby, E. Flynt, A. Hoering, S.K. Johnson, M.W. Rutherford, C.P. Wardell, M.A. Bauer, C. Dumontet, T. Facon, C.D. Schinke, M. Zangari, F. van Rhee, B. Barlogie, D. Cairns, G. Jackson, A. Thakurta, F.E. Davies, G.J. Morgan, B.A. Walker
Administrative, technical, or material support (i.e., reporting or organizing data, constructing databases): S. Deshpande, H. Wang, Y. Wang, M.W. Rutherford, C. Dumontet, B. Barlogie, G.J. Morgan
Study supervision: B.A. Walker
Other (sample processing): R.G. Tytarenko

Acknowledgments

E.M. Boyle received funding from the Fédération Française de Recherche sur le Myélome et les Gammapathies under the aegis of the Fondation de France. This work was supported by a Leukemia and Lymphoma Translational Research Program grant #6602-20 (to B.A. Walker). The authors would like to thank Dr. Jill Corre (Toulouse) for her help regarding the IFM-2009 model.

The costs of publication of this article were defrayed in part by the payment of page charges. This article must therefore be hereby marked *advertisement* in accordance with 18 U.S.C. Section 1734 solely to indicate this fact.

Received May 8, 2019; revised October 11, 2019; accepted January 22, 2020; published first January 27, 2020.

References

1. SEER Data. Cancer stat facts: myeloma [Internet]. National Cancer Institute. [cited 2018]. Available from: https://seer.cancer.gov/statfacts/html/mulmy.html.
2. Lonial S, Boise LH, Kaufman J. How I treat high-risk myeloma. Blood 2015;126:1536–43.
3. Walker BA, Mavrommatis K, Wardell CP, Ashby TC, Bauer M, Davies F, et al. A high-risk, Double-Hit, group of newly diagnosed myeloma identified by genomic analysis. Leukemia 2018;33:159–70.
4. Walker BA, Boyle EM, Wardell CP, Murison A, Begum DB, Dahir NM, et al. Mutational spectrum, copy number changes, and outcome: results of a sequencing study of patients with newly diagnosed myeloma. J Clin Oncol 2015;33:3911–20.
5. Magrangeas F, Avet-Loiseau H, Gouraud W, Lodé L, Decaux O, Godmer P, et al. Minor clone provides a reservoir for relapse in multiple myeloma. Leukemia 2013;27:473–81.
6. Egan JB, Shi C-X, Tembe W, Christoforides A, Kurdoglu A, Sinari S, et al. Whole-genome sequencing of multiple myeloma from diagnosis to plasma cell leukemia reveals genomic initiating events, evolution, and clonal tides. Blood 2012;120:1060–6.
7. Sawyer JR, Tian E, Heuck CJ, Epstein J, Johann DJ, Swanson CM, et al. Jumping translocations of 1q12 in multiple myeloma: a novel mechanism for deletion of 17p in cytogenetically defined high-risk disease. Blood 2014;123:2504–12.
8. Walker BA, Mavrommatis K, Wardell CP, Ashby TC, Bauer M, Davies FE, et al. Identification of novel mutational drivers reveals oncogene dependencies in multiple myeloma. Blood 2018;132:587–97.
9. Hoang PH, Dobbins SE, Cornish AJ, Chubb D, Law PJ, Kaiser M, et al. Whole-genome sequencing of multiple myeloma reveals oncogenic pathways are targeted somatically through multiple mechanisms. Leukemia 2018;32:2459–70.
10. Bolli N, Avet-Loiseau H, Wedge DC, Van Loo P, Alexandrov LB, Martincorena I, et al. Heterogeneity of genomic evolution and mutational profiles in multiple myeloma. Nat Commun 2014;5:2997.
11. Bolli N, Biancon G, Moarii M, Gimondi S, Li Y, de Philippis C, et al. Analysis of the genomic landscape of multiple myeloma highlights novel prognostic markers and disease subgroups. Leukemia 2018;32:2604–16.
12. Johnson DC, Lenive O, Mitchell J, Jackson G, Owen R, Drayson M, et al. Neutral tumor evolution in myeloma is associated with poor prognosis. Blood 2017;130:1639–43.
13. Walker BA, Wardell CP, Johnson DC, Kaiser MF, Begum DB, Dahir NB, et al. Characterization of IGH locus breakpoints in multiple myeloma indicates a subset of translocations appear to occur in pregerminal center B cells. Blood 2013;121:3413–9.
14. Walker BA. Whole exome sequencing in multiple myeloma to identify somatic single nucleotide variants and key translocations involving immunoglobulin loci and MYC. In: Heuck C, Weinhold N, editors. Multiple myeloma: methods and protocols. New York, NY: Springer New York; 2018. p.71–95.
15. Thakurta A, Ortiz M, Blecua P, Towfic F, Corre J, Serbina NV, et al. High subclonal fraction of 17p deletion is associated with poor prognosis in multiple myeloma. Blood 2019;133:1217–21.
16. Zhou Y, Zhang Q, Stephens O, Heuck CJ, Tian E, Sawyer JR, et al. Prediction of cytogenetic abnormalities with gene expression profiles. Blood 2012;119:e148–150.
17. The Jackson Laboratory. The clinical knowledgebase (CKB); 2019. Available from: https://ckb.jax.org/.

18. Walker BA, Wardell CP, Murison A, Boyle EM, Begum DB, Dahir NM, et al. APOBEC family mutational signatures are associated with poor prognosis translocations in multiple myeloma. Nat Commun 2015;6:6997.
19. Dankner M, Rose AAN, Rajkumar S, Siegel PM, Watson IR. Classifying BRAF alterations in cancer: new rational therapeutic strategies for actionable mutations. Oncogene 2018;37:3183.
20. Perrot A, Lauwers-Cances V, Tournay E, Hulin C, Chretien M-L, Royer B, et al. Development and validation of a cytogenetic prognostic index predicting survival in multiple myeloma. J Clin Oncol 2019;37:1657–65.
21. Boyle EM, Proszek PZ, Kaiser MF, Begum D, Dahir N, Savola S, et al. A molecular diagnostic approach able to detect the recurrent genetic prognostic factors typical of presenting myeloma. Genes Chromosomes Cancer 2015;54:91–8.
22. Barrio S, DáVia M, Bruins L, Stühmer T, Steinbrunn T, Bittrich M, et al. Protocol for M3P: a comprehensive and clinical oriented targeted sequencing panel for routine molecular analysis in multiple myeloma. Methods Mol Biol 2018;1792:117–28.
23. Bolli N, Li Y, Sathiaseelan V, Raine K, Jones D, Ganly P, et al. A DNA target-enrichment approach to detect mutations, copy number changes and immunoglobulin translocations in multiple myeloma. Blood Cancer J 2016;6:e467–e467.
24. He J, Abdel-Wahab O, Nahas MK, Wang K, Rampal RK, Intlekofer AM, et al. Integrated genomic DNA/RNA profiling of hematologic malignancies in the clinical setting. Blood 2016;127:3004–14.
25. Attal M, Harousseau J-L, Stoppa A-M, Sotto J-J, Fuzibet J-G, Rossi J-F, et al. A prospective, randomized trial of autologous bone marrow transplantation and chemotherapy in multiple myeloma. N Engl J Med 1996;335:91–7.
26. Harousseau JL, Milpied N, Laporte JP, Collombat P, Facon T, Tigaud JD, et al. Double-intensive therapy in high-risk multiple myeloma. Blood 1992;79:2827–33.
27. Barlogie B, Jagannath S, Desikan KR, Mattox S, Vesole D, Siegel D, et al. Total therapy with tandem transplants for newly diagnosed multiple myeloma. Blood 1999;93:55–65.
28. Attal M, Harousseau J-L, Facon T, Guilhot F, Doyen C, Fuzibet J-G, et al. Single versus double autologous stem-cell transplantation for multiple myeloma. N Engl J Med 2003;349:2495–502.
29. Björkstrand B. European Group for Blood and Marrow Transplantation Registry studies in multiple myeloma. Semin Hematol 2001;38:219–25.
30. COSMIC. COSMIC—Catalogue of Somatic Mutations in Cancer. Available from: https://cancer.sanger.ac.uk/cosmic.
31. Marchetti A, Felicioni L, Malatesta S, Grazia Sciarrotta M, Guetti L, Chella A, et al. Clinical features and outcome of patients with non–small cell lung cancer harboring BRAF mutations. J Clin Oncol 2011;29:3574–9.
32. Andrulis M, Lehners N, Capper D, Penzel R, Heining C, Huellein J, et al. Targeting the BRAF V600E mutation in multiple myeloma. Cancer Discov 2013;3:862–9.
33. Rustad EH, Dai HY, Hov H, Coward E, Beisvag V, Myklebost O, et al. BRAF V600E mutation in early-stage multiple myeloma: good response to broad acting drugs and no relation to prognosis. Blood Cancer J 2015;5:e299.
34. Litvak AM, Paik PK, Woo KM, Sima CS, Hellmann MD, Arcila ME, et al. Clinical characteristics and course of 63 patients with BRAF mutant lung cancers. J Thorac Oncol 2014;9:1669–74.
35. Tissot C, Couraud S, Tanguy R, Bringuier P-P, Girard N, Souquet P-J. Clinical characteristics and outcome of patients with lung cancer harboring BRAF mutations. Lung Cancer 2016;91:23–8.
36. Lionetti M, Barbieri M, Todoerti K, Agnelli L, Marzorati S, Fabris S, et al. Molecular spectrum of BRAF, NRAS and KRAS gene mutations in plasma cell dyscrasias: implication for MEK-ERK pathway activation. Oncotarget 2015;6:24205–17.
37. Wan PTC, Garnett MJ, Roe SM, Lee S, Niculescu-Duvaz D, Good VM, et al. Mechanism of activation of the RAF-ERK signaling pathway by oncogenic mutations of B-RAF. Cell 2004;116:855–67.
38. Haling JR, Sudhamsu J, Yen I, Sideris S, Sandoval W, Phung W, et al. Structure of the BRAF-MEK complex reveals a kinase activity independent role for BRAF in MAPK signaling. Cancer Cell 2014;26:402–13.
39. Richtig G, Hoeller C, Kashofer K, Aigelsreiter A, Heinemann A, Kwong LN, et al. Beyond the BRAFV600E hotspot: biology and clinical implications of rare BRAF gene mutations in melanoma patients. Br J Dermatol 2017;177:936–44.
40. Bohn OL, Hsu K, Hyman DM, Pignataro DS, Giralt S, Teruya-Feldstein J. BRAF V600E mutation and clonal evolution in a patient with relapsed refractory myeloma with plasmablastic differentiation. Clin Lymphoma Myeloma Leuk 2014;14:e65–8.
41. Sharman JP, Chmielecki J, Morosini D, Palmer GA, Ross JS, Stephens PJ, et al. Vemurafenib response in 2 patients with posttransplant refractory BRAF V600E-mutated multiple myeloma. Clin Lymphoma Myeloma Leuk 2014;14:e161–3.
42. Hyman DM, Puzanov I, Subbiah V, Faris JE, Chau I, Blay J-Y, et al. Vemurafenib in multiple nonmelanoma cancers with BRAF V600 mutations. N Engl J Med 2015;373:726–36.
43. Sánchez-Torres JM, Viteri S, Molina MA, Rosell R. BRAF mutant non–small cell lung cancer and treatment with BRAF inhibitors. Transl Lung Cancer Res 2013;2:244–50.
44. Binder M, Rajkumar SV, Ketterling RP, Greipp PT, Dispenzieri A, Lacy MQ, et al. Prognostic implications of abnormalities of chromosome 13 and the presence of multiple cytogenetic high-risk abnormalities in newly diagnosed multiple myeloma. Blood Cancer J 2017;7:e600.
45. Avet-Loiseau H, Garand R, Lodé L, Harousseau J-L, Bataille R. Translocation t(11;14)(q13;q32) is the hallmark of IgM, IgE, and nonsecretory multiple myeloma variants. Blood 2003;101:1570–1.
46. Pertesi M, Vallée M, Wei X, Revuelta MV, Galia P, Demangel D, et al. Exome sequencing identifies germline variants in DIS3 in familial multiple myeloma. Leukemia 2019;33:2324–30.
47. Milbury KL, Paul B, Lari A, Fowler C, Montpetit B, Stirling PC. Exonuclease domain mutants of yeast DIS3 display genome instability. Nucl Austin Tex 2019;10:21–32.
48. Tomecki R, Drazkowska K, Kucinski I, Stodus K, Szczesny RJ, Gruchota J, et al. Multiple myeloma-associated hDIS3 mutations cause perturbations in cellular RNA metabolism and suggest hDIS3 PIN domain as a potential drug target. Nucleic Acids Res 2014;42:1270–90.